Spectroscopic study of a possible math xmlns="http://www.w3.org/1998/Math/MathML">mrow>mi mathvariant="normal">Λ/mi>mi>n/mi>mi>n/mi>/mrow>/ math> resonance and a pair of math xmlns="http://www.w3.org/1998/Math/MathML">mrow>mi mathvariant="normal">Σ/mi>mi>N/mi>mi>N/mi>/mrow> /math> states using the math xmlns="http://www.w3.org/1998/Math/MathML">mrow>mo >(/mo>mi>e/mi>mo>,/mo>msup>mi>e/mi>mo>′/mo>/ msup>msup>mi>K/mi>mo>+/mo>/msup>mo>)/mo>/mr ow>/math> reaction with a tritium target

B. Pandey et al. (Hall A Collaboration)

Phys. Rev. C **105**, L051001 — Published 20 May 2022

DOI: 10.1103/PhysRevC.105.L051001

Spectroscopic study of a possible Λnn resonance and a pair of ΣNN states using the $(e, e'K^+)$ reaction with a tritium target

B. Pandey,[1] L. Tang,[1,2,*] T. Gogami,[3,4] K.N. Suzuki,[4] K. Itabashi,[3] S. Nagao,[3] K. Okuyama,[3] S.N. Nakamura,[3] D. Abrams,[5] I. R. Afnan,[6] T. Akiyama,[3] D. Androic,[7] K. Aniol,[8] T. Averett,[9] C. Ayerbe Gayoso,[9] J. Bane,[10] S. Barcus,[9] J. Barrow,[10] V. Bellini,[11] H. Bhatt,[12] D. Bhetuwal,[12] D. Biswas,[1] A. Camsonne,[2] J. Castellanos,[13] J-P. Chen,[2] J. Chen,[9] S. Covrig,[2] D. Chrisman,[14,15] R. Cruz-Torres,[16] R. Das,[17] E. Fuchey,[18] C. Gal,[5] B. F. Gibson,[19] K. Gnanvo,[5] F. Garibaldi,[11,20] T. Gautam,[1] J. Gomez,[2] P. Gueye,[1] T.J. Hague,[21] O. Hansen,[2] W. Henry,[2] F. Hauenstein,[22] D. W. Higinbotham,[2] C. Hyde,[22] M. Kaneta,[3] C. Keppel,[2] T. Kutz,[17] N. Lashley-Colthirst,[1] S. Li,[23,24] H. Liu,[25] J. Mammei,[26] P. Markowitz,[13] R. E. McClellan,[2] F. Meddi,[11] D. Meekins,[2] R. Michaels,[2] M. Mihovilovič,[27,28,29] A. Moyer,[30] D. Nguyen,[16,31] M. Nycz,[21] V. Owen,[9] C. Palatchi,[5] S. Park,[17] T. Petkovic,[7] S. Premathilake,[5] P. E. Reimer,[32] J. Reinhold,[13] S. Riordan,[32] V. Rodriguez,[33] C. Samanta,[34] S.N. Santiesteban,[23] B. Sawatzky,[2] S. Širca,[27,28] K. Slifer,[23] T. Su,[21] Y. Tian,[35] Y. Toyama,[3] K. Uehara,[3] G.M. Urciuoli,[11] D. Votaw,[14,15] J. Williamson,[36] B. Wojtsekhowski,[2] S. Wood,[2] B. Yale,[23] Z. Ye,[32] J. Zhang,[5] and X. Zheng[5]

(Hall A Collaboration)

[1] *Department of Physics, Hampton University, Virginia 23668, USA*
[2] *Thomas Jefferson National Accelerator Facility, Newport News, Virginia 23606, USA*
[3] *Graduate School of Science, Tohoku University, Sendai, Miyagi 980-8578, Japan*
[4] *Graduate School of Science, Kyoto University,Kyoto 606-8502, Japan*
[5] *Department of Physics, University of Virginia, Charlottesville, Virginia 22904, USA*
[6] *School of Chemical and Physical Science, Flinders University, GPO Box 2100, Adelaide 5001, Australia*
[7] *Department of Physics & Department of Applied Physics, University of Zagreb, HR-10000 Zagreb, Croatia*
[8] *Physics and Astronomy Department, California State University, Los Angeles, California 90032, USA*
[9] *Department of Physics, The College of William and Mary, Virginia 23185, USA*
[10] *Department of Physics, University of Tennessee, Knoxville, Tennessee 37996, USA*
[11] *INFN, Sezione di Roma, 00185, Rome, Italy*
[12] *Department of Physics, Mississippi State University, Mississippi State, Mississippi 39762, USA*
[13] *Department of Physics, Florida International University, Miami, Florida 33199, USA*
[14] *Department of Physics and Astronomy, Michigan State University, East Lansing, Michigan 48824, USA*
[15] *National Superconducting Cyclotron Laboratory, Michigan State University, East Lansing, MI 48824, USA*
[16] *Department of Physics, Massachusetts Institute of Technology, Cambridge, Massachusetts 02139, USA*
[17] *Department of Physics, State University of New York, Stony Brook, New York 11794, USA*
[18] *Department of Physics, University of Connecticut, Storrs, Connecticut 06269, USA*
[19] *Theoretical Division, Los Alamos National Laboratory, Los Alamos, New Mexico 87545, USA*
[20] *Istituto Superiore di Sanità, 00161, Rome, Italy*
[21] *Department of Physics, Kent State University, Kent, Ohio 44242, USA*
[22] *Department of Physics, Old Dominion University, Norfolk, Virginia 23529, USA*
[23] *Department of Physics, University of New Hampshire, Durham, New Hampshire 03824, USA*
[24] *Nuclear Science Division, Lawrence Berkeley National Laboratory, Berkeley, CA 94720, USA*
[25] *Department of Physics, Columbia University, New York, New York 10027, USA*
[26] *Department of Physics and Astronomy, University of Manitoba, Winnipeg, Manitoba R3T 2N2, Canada*
[27] *Faculty of Mathematics and Physics, University of Ljubljana, 1000 Ljubljana, Slovenia*
[28] *Jožef Stefan Institute, Ljubljana, Slovenia*
[29] *Institut für Kernphysik, Johannes Gutenberg-Universität Mainz, DE-55128 Mainz, Germany*
[30] *Department of Physics, Christopher Newport University, Newport News, Virginia 23606, USA*
[31] *University of Education, Hue University, Hue City, Vietnam*
[32] *Physics Division, Argonne National Laboratory, Lemont, Illinois 60439, USA*
[33] *División de Ciencias y Tecnologia, Universidad Ana G. Méndez, Recinto de Cupey, San Juan 00926, Puerto Rico*
[34] *Department of Physics & Astronomy, Virginia Military Institute, Lexington, Virginia 24450, USA*
[35] *Department of Physics, Syracuse University, New York, New York 10016, USA*
[36] *School of Physics & Astronomy, University of Glasgow, Glasgow, G12 8QQ, Scotland, UK*

(Dated: May 13, 2022)

A mass spectroscopy experiment with a pair of nearly identical high resolution spectrometers and a tritium target was performed in Hall A at Jefferson Lab. Utilizing the $(e, e'K^+)$ reaction, enhancements, which may correspond to a possible Λnn resonance and a pair of ΣNN states, were observed with an energy resolution of about 1.21 MeV (σ), although greater statistics are needed to make definitive identifications. An experimentally measured Λnn state may provide a unique constraint in determining the Λn interaction, for which no scattering data exist. In addition, although bound A = 3 and 4 Σ hypernuclei have been predicted, only an A = 4 Σ hypernucleus

($^4_\Sigma$He) was found, utilizing the (K^-, π^-) reaction on a ^{4}He target. The possible bound ΣNN state is likely a $\Sigma^0 nn$ state, although this has to be confirmed by future experiments.

A primary goal of nuclear physics is to investigate and understand the behavior of strongly interacting nuclear many-body systems, from few-body nuclei to neutron stars, in terms of the baryonic interactions. Currently, the most commonly utilized baryon-baryon interaction models (Nijmegen [1–4] or Jülich [5, 6]) are based on extensive NN scattering data but an extremely limited set of data involving other baryons. In the case of the ΛN interaction, there are just several hundred Λp events that spread over a large momentum range, while there are no Λn data. As a result, there is only a limited constraint on the ΛN interaction, and one must assume that charge symmetry holds. To overcome this limitation, the properties of hypernuclei have been used to model charge symmetry breaking (CSB) in the ΛN interaction.

Recent high precision spectroscopy on the binding energy of the 0^+ ground state of $^4_\Lambda$H [7, 8] and the energy of the γ transition between the 1^+ first excited state and 0^+ ground state of $^4_\Lambda$He [9] determine the Λ separation energy difference between the ground states of $^4_\Lambda$H and $^4_\Lambda$He to be 0.233 ± 0.092 MeV. This CSB in the ΛN interaction suggested by the pair of A = 4 hypernuclei is surprisingly several times larger than that observed in the nuclear ^{3}H$-^3$He isodoublet pair (< 0.10 MeV) due to CSB in the NN interaction after the Coulomb correction. This suggests that the charge symmetry assumed in equating the Λp and Λn interactions needs to be reexamined experimentally by measurements of the Λn amplitude.

Recently, the HypHI experiment at GSI [10] suggested a possible observation of a neutral bound $^3_\Lambda n$ system (a Λ coupled to a di-neutron system). However, several theoretical analyses concluded that such a bound state cannot exist [11–13] based upon our current understanding of the ΛN interaction and the observed properties of hypernuclei. In contrast, a theoretical investigation [14, 15] took an alternative approach aiming to investigate what might be learned from the existence of a Λnn three-body resonance, using separable nn and Λn potentials in a Faddeev-type analysis. It concluded that a physical three-body Λnn resonance can exist with as little as an $\approx$ 5% Λn strength increase over the initial $\Lambda n = \Lambda p$ strength hypothesis. Thus, an observation of a $^3_\Lambda n$ resonance with good precision can provide significant constraints in determining properties of the Λn interaction.

A mass spectroscopy study using the $(e, e'K^+)$ reaction with a tritium (^{3}H) target and the high quality CEBAF beam at JLab should be a unique opportunity for such an investigation. Taking advantage of a group of approved and running experiments that shared a common pressurized tritium gas (T_2) target in Hall A, the experiment (E12-17-003) was carried out [16], although the available experimental conditions and kinematics were not optimized for producing hypernuclei using the $(e, e'K^+)$ reaction.

The energy of the continuous wave electron beam for the experiment was 4.326 GeV and its energy stability and spread were controlled to be at a level of $\Delta E/E \approx 6.5 \times 10^{-5}$. The beam size was tuned to be $\approx$ 200 μm in diameter but smeared to a larger size to protect the target by a fast beam raster system. Using the beam position measurements along the beam line and the raster frequency and phase angle, the raster correction was performed in the data analysis to ensure an accurate knowledge of beam coordinates in the X-Y plane perpendicular to the beam direction.

A pair of high-resolution spectrometers (HRS) [17] were symmetrically positioned with respect to the beam (left and right in the horizontal plane) at a forward angle of 13.2°. Each HRS has $\approx \pm$ 4% momentum acceptance and $\approx$ 6 msr solid angle acceptance. The left HRS (LHRS) with its central momentum set at 2.218 GeV/c was used to detect and analyze the scattered electron. The virtual photon momentum vector was then in the direction of the right HRS (RHRS) used to detect the positively charged kaon, associatively produced with either a Λ or Σ^0 (or Σ^-) from a proton (or a neutron) in the target nucleus (except hydrogen). The kaon was thus emitted at or near zero degrees w.r.t. the virtual photon, maximizing the photo-production cross section. The RHRS central momentum was set at 1.823 GeV/c to give an $\approx$ 15% survival rate for the short-lived kaon (due to a full path length of $\approx$ 26 m). This configuration maximized the kinematic acceptance around the threshold mass region of $^3_\Lambda n$. Both the corresponding -Q^2 and 3-momentum transfer to the recoil Λ (or Σ) are high, ≈ 0.5 (GeV/c)^2 and $\approx$ 400 MeV/c, respectively. These kinematic conditions lowered the virtual photon flux and the hypernuclear photo-production cross section, the production yield was small.

The detector package for each HRS consisted of a pair of vertical drift chambers (VDC) placed along the titled focal plane for measurement of the focal plane coordinates, followed by two scintillation detectors for timing and providing trigger signals. For the LHRS a CO_2 gas Čerenkov (positioned behind the scintillation detectors) was used to separate scattered electrons and negatively charged pions. For the RHRS two layers of Aerogel Čerenkov counters with different refractive indices were installed between the two scintillation detectors for the kaon identification. The one with low index (n = 1.015) was used to separate positively charged pions and positrons from kaons and protons, while the one with higher index ($n = 1.05$) was used to reject protons.

The event coordinates are defined from the center of the targets with z pointing along the beam direction (x

* Corresponding author. tangl@jlab.org

points to the left and y points up). The pressurized Tritium (84.8 $\pm$ 0.8 mg/cm^2) and Hydrogen (70.8 $\pm$ 0.4 mg/cm^2) gases were sealed in identical cylindrical aluminum cells which were 25 cm long and 1.27 cm in diameter [18]. The energy straggling was dominantly from the cylindrical side wall with $\approx$ 400 μm average thickness. The energy and momentum loss uncertainties due to path length variation and wall thickness non-uniformity dominated the systematic uncertainty of the reconstructed missing mass [16]. The experiment also used a multi-foil target, with 11 thin carbon foils spaced by 2.5 cm along 25 cm in the z direction, and an empty cell target.

The data separately collected by each HRS from the multi-foil target were used to optimize the z-vertex reconstruction matrix with the measured focal plane coordinates and the known target position. For the coincidence data, the difference between the two independently reconstructed z's provided a coincidence spectrum of the reaction positions. The $(e, e'K^+)$ events were selected from the coincidence peak. Then the average of the two z's was used as the target z. A resolution of $\sigma_z \approx 4$ mm was achieved. A z-vertex gate ranging from -10 cm to +10 cm was applied to select the events from the gas region. By applying the same gate to the data collected from the empty cell target, the events leaked from the end caps were found to be less than $\approx 1\%$, thus having negligible contribution to the background.

The angle reconstruction matrices, which determine the in-plane and out-of-plane scattering angles by the measured focal plane coordinates and scattering coordinate z, were calibrated and optimized by particles emitted from the multi-foil target through suited sieve slit plates. These plates, located 1.03 meters away from the center of the target at $z = 0$, were equipped with 4 mm diameter holes, which defined specific pairs of the in-plane and out-of-plane angles w.r.t. the spectrometer central axis. Using the optimized matrices (each up to fourth order), the resolutions for the in-plane and out-of-plane angles were estimated to be about 1.7 mrad and 2.4 mrad in σ, respectively. The polar angle resolution, with z along the beam direction, was estimated to be $\sigma_\theta \approx 2.4$ mrad.

Figure 1 shows the coincidence time spectrum between the scattered electrons (e') and the emitted kaons (K^+), obtained by ΔT = T(LHRS) - T(RHRS). The CEBAF's beam bunch separation is 2 ns. Taking into account the flight path-length and velocity dependences with the kaon mass, a time resolution of $\sigma_t \approx 0.3$ ns was achieved. The pions and protons are due to the inefficiency of the aerogel detectors and caused the accidental background.

By reducing the central momentum of the LHRS to 2.10 GeV/c, the kinematic acceptance was shifted so that data taken with this H run condition insured that both the peaks of Λ and Σ^0 electro-produced from the H_2 target appeared together in the missing mass spectrum [16]. Their known masses were utilized to ensure the precision of the absolute missing mass scale, while their widths were used to optimize the momentum reconstruction matrices (each up to fifth order) of the LHRS and RHRS.

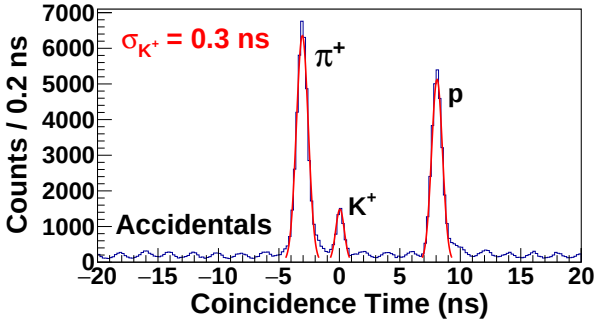

FIG. 1. (Color online) The coincidence time between LHRS (e') and RHRS (K^+). The coincident pions and protons were due to the inefficiency of the two aerogel detectors and caused the accidental background.

This technique was successfully applied by all previous high precision hypernuclear mass spectroscopy experiments using the $(e, e'K^+)$ reaction carried out in JLab Hall C [19]. However, as is known in electron elastic scattering from a proton, the momentum of the scattered electron has a strong scattering angle dependence. Thus, the momentum uncertainty has a contribution from the kinematic angular uncertainty in addition to the momentum reconstruction resolution. Similarly, in case of Λ and Σ^0 production from H using the $(e, e'K^+)$ reaction, their peak widths in the missing mass spectrum have non-negligible contributions from the angular resolution of the outgoing electrons and kaons. The reconstructed momentum matrices cannot be fully optimized by only minimizing the peak width of the Λ and Σ^0 produced from H. A simulation study demonstrated that contributions from the angular uncertainties become negligible when the target is sufficiently heavy (A $>$ 7). Then the peak width of a defined missing mass depends only on the momentum resolution of the two spectrometers. Therefore, incorporating a heavier hypernucleus will improve the momentum matrix optimization, while including the Λ and Σ^0 provides the calibration of the absolute mass scale. This method was not applied in the analysis for the cross section measurement reported in Ref. [16].

The events observed from the entrance and exit aluminum caps were analyzed for the electro-produced $^{27}_{\Lambda}$Mg hypernuclei. Although statistics were very low, a peak search analysis found three peaks that likely correspond to the Λ in the s-, p- and d-orbits coupled to the core-nucleus in the ground or low-lying states. The momentum matrices were optimized by minimizing the peak widths of these three peaks with higher statistical weights and simultaneously that of the Λ and Σ^0 from the H_2 target with lower weights. The iterative optimization process ended when the width of the $^{27}_{\Lambda}$Mg ground state appeared to be 1.28 $\pm$ 0.3 MeV (σ), in agreement with the width given by the simulation. The result showed that the widths of the Λ and Σ^0 were 1.35 $\pm$ 0.05 MeV (σ) and 1.32 $\pm$ 0.09 MeV (σ), respectively, also agreeing well with the simulation prediction, and their recon-

structed masses agreed with the known values within ± 0.05 MeV. The binding energy of the $^{27}_{\Lambda}$Mg ground state (Λ_s) appeared to be -B_Λ ≈ -13.55 ± 0.3 MeV MeV, while that of the two excited states (Λ_p and Λ_d) were -2.45 ± 0.6 MeV and 6.45 ± 0.5 MeV, respectively. Since the absolute mass scale was calibrated by the Λ and Σ^0 from the gas target H while the absolute mass after energy loss corrections for the events from the two aluminum caps could not be determined precisely, there could be a kinematic offset as large as about ± 1.5 MeV for the binding energy scale of $^{27}_{\Lambda}$Mg. The resolution for the A = 3 hypernucleus was then predicted to be about 1.21 MeV (σ) which is slightly better than both that for the A = 1 and 27 systems. This is because the mass A = 3 falls in the region where the contribution from the angular uncertainties decreased dramatically near the minimum while that from the uncertainties of energy and momenta had not yet reached the maximum.

For the data from the T_2 target, there was about a 3% ^{3}He contamination due mainly to the beta decay of ^{3}H, which generated a low, broad distribution in the combined Λ and Σ quasi-free production. More importantly, as proven by other tritium experiments, there was also a small H_2 contamination which generates a free Λ peak in the Λ*nn* spectrum. To estimate this, the T data were analyzed assuming the proton target mass, as shown in Fig. 2. Above the known accidental background and the broad distribution that combines both the Λ and Σ quasi-free production, and the ^{3}He contamination (all with the wrong kinematics), there is a clear free Λ peak. The function for the broad distribution was obtained by using the SIMA simulation with the available ^{3}He spectral function [20]. Using the known distribution function fitted from the Λ peak in the H data, the amplitudes of the two functions were fitted and the total number of free Λ events was then estimated to be about 158 counts based on the number of events above the fitted quasi-free distribution. Data were also taken with the H_2 target under the T_2 target run condition. These data were analyzed using both the H and T kinematics. With the correct kinematics, the Λ peak provided confirmation of resolution and missing mass scale. With the incorrect kinematics, the free Λ peak in the Λ*nn* spectrum was, as expected, significantly broadened, and its distribution as a function of the Λ binding energy B_Λ in the Λ*nn* system was obtained, see Fig. 3.

Analyzed with the optimized matrices, the T data (see Fig. 4) exhibit a missing mass spectrum plotted in terms of the binding energy B_Λ of the $^3_\Lambda n$ hypernucleus with the threshold mass defined as the rest mass of the Λ*nn* system. The overall spectrum (red solid line) can be interpreted as coming from five dominant contributions, I: the precisely measured accidental background (dark green cross); II: the known free Λ distribution but scaled down for 158 counts (blue solid-line); III: the 3% ^{3}He contamination (simulated by SIMA); IV and V: the quasi-free production of Λ (red dashed line) and the combination of Σ^0 and Σ^- (above the tail of the Λ quasi-free) which

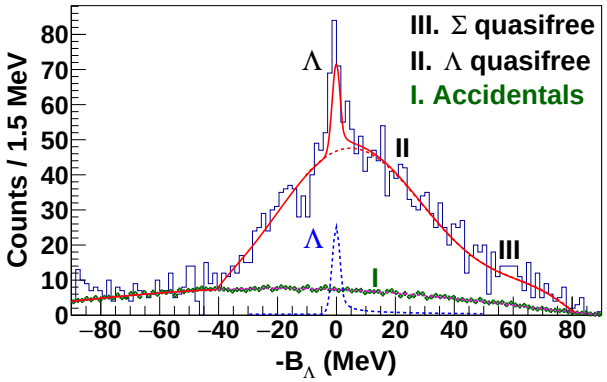

FIG. 2. (Color online) The missing mass spectrum obtained from the T data but analyzed using the H kinematics. A clear free Λ peak from the H_2 contamination can be seen at B_Λ = 0 above a broad distribution that combines the accidental and ^{3}He contamination backgrounds and the Λ and Σ quasi-free productions estimated by the SIMA simulation with the existing three-body (^{3}He) spectral function [20].

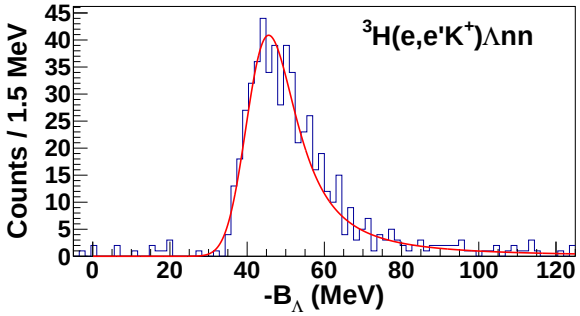

FIG. 3. (Color online) Spectra from the H data taken under the T run condition. The distribution function for the expected free Λ peak in terms of the Λ binding energy in the Λ*nn* system is precisely obtained.

were simulated by the SIMA code with the available ^{3}He spectral function. The amplitudes of the quasi-free distributions were obtained by the best fit for the overall distribution. The two vertical black dashed lines show the Σ*NN* thresholds (the $\Sigma^- d$ threshold lies in about the middle but is omitted here. Final state interactions were not included in the SIMA simulation. Here, the spectral functions for ^{3}H and ^{3}He are not identical. Therefore, the quasi-free distributions described may not be precise, but are considered to be close.

Over the range from -B_Λ = - 6 MeV to 38 MeV, one observes a possible peak at the Λ*nn* threshold and broad extra strength above the predicted distribution. Due to low statistics and relatively high background, precise fitting of the peak at the threshold alone was difficult. Therefore, the spectrum was fitted by introducing two Gaussian functions: one for the small peak at threshold, and a broad one for the extra strength appearing above the predicted distribution, as shown in the enlarged view in Fig. 5. The predicted distribution that includes the acci-

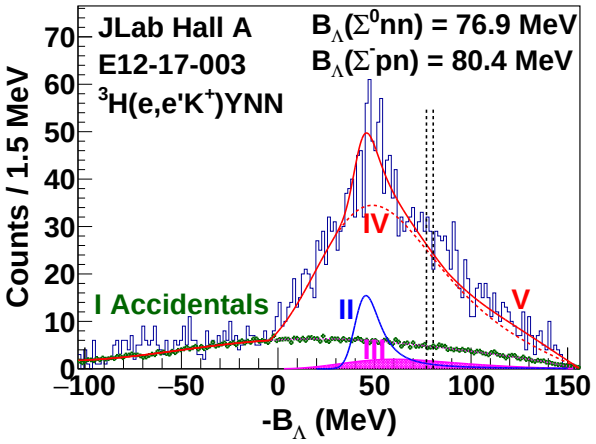

FIG. 4. (Color online) The mass spectrum in terms of the binding energy B_Λ of the ${}^3_\Lambda n$ hypernucleus. The dominant contributions are from, I: the known accidentals; II: the free $\Lambda's$ from the known H_2 contamination; III: the known ^{3}He contamination; IV: the Λ quasi-free production (red dash-line with I and III included); and V: the combined Σ^0 and Σ^- quasi-free productions (above the tail of IV). The two vertical black dash-lines show the two ΣNN thresholds.

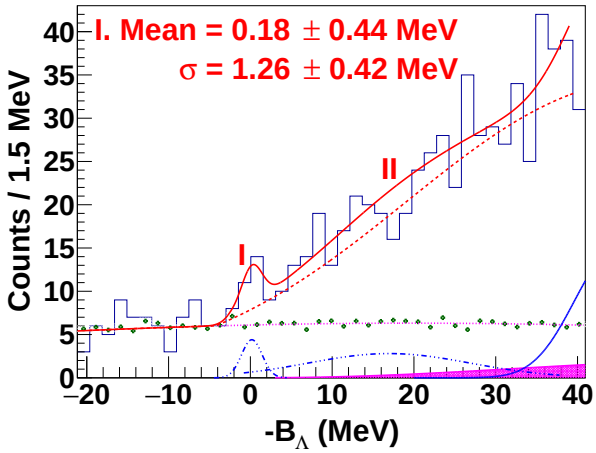

FIG. 5. (Color online) The enlarged mass spectrum around the Λnn threshold. Two additional Gaussians were fitted together with the known contributions (the accidentals, the Λ quasi-free, the free Λ, and the ^{3}He contamination). The one at the threshold is for the small peak, while the broad one is for the additional strength above the predicted quasi-free distribution.

dental background, the quasi-free Λ production from T, the free Λ production from the H_2 contamination, and the ^{3}He contamination was treated as known. The χ^2/ndf was found to be about 0.9. The extra strength may come from the incorrect ^{3}He spectral function or from the unknown final state interactions that were not included in the simulation. The small peak appears to have $-B_\Lambda$ = 0.18 ± 0.44 (stat) ± 0.4 (sys) MeV with a width of σ = 1.26 ± 0.42 MeV (stat) ± 0.5 (sys) MeV. Deconvolving the intrinsic resolution (σ = 1.21 MeV) predicted for the A = 3 system, the natural width ($\Gamma/2$) seems to be ≈ 0.35 MeV. This may possibly be the ${}^3_\Lambda n$ state for which the experiment was searching. However, after including the estimated radiative corrections, the statistical significance, simply calculated as the ratio of the signal over the square root of the sum of the signal and background, is only about 2.7 over a ± 2.0 σ width range. It is not sufficient to permit a definite identification. If this state does exist, its differential cross section was estimated to be about 10 nb/sr [16]. The high 3-momentum transfer (≈ 400 MeV/c) to the Λ increases the probability that the Λ will dissociate from the recoil nucleus.

Another interesting observation is the excess of events above the Λ quasi-free distribution around the Σ thresholds. Due to the limited momentum acceptance of the two HRS spectrometers, the experimental kinematics was chosen to maximize the kinematic acceptance around the missing mass of the Λnn threshold ($-B_\Lambda$ = 0). Starting from about $-B_\Lambda$ = 60 MeV, the kinematic acceptance decreases so that the events from the Σ quasi-free productions were removed as the missing mass increases. Thus, the spectrum in the Σ threshold region suffered less influence from the Σ quasi-free distribution. Two broad enhancements are visible. Figure 6 is an enlarged view for the Σ production region with a larger bin size to reduce the statistical fluctuation. The first enhancement appears at about 3.14 ± 0.84 MeV below the $\Sigma^0 nn$ threshold with a width of $\sigma \approx$ 2.28 ± 1.2 MeV. The second one appears above these thresholds about 13.3 MeV away from the first one. The $\Sigma^- d$ threshold is in about the middle of the two and is not shown here. The two enhancements have statistical significances of about 2.2 and 4.6 and cross sections of about 20 nb/sr and 50 nb/sr, respectively. The first enhancement possibly hints at a bound Σnn (I = 1) state, while the second may be an excited ΣNN state. However, since the spectral functions for ^{3}H and ^{3}He are different, the predicted quasi-free distributions may not be accurate. This may affect the interpretation of this observation.

Although predictions for bound A = 3 [21] and 4 Σ hypernuclei exist, only an A = 4 Σ hypernucleus (${}^4_\Sigma$He) was so far experimentally found [22], by means of the (K^-, π^-) reaction on a He target at the BNL-AGS. Because the Σ^+ production threshold is the lowest, it was claimed to be a bound Σ^+ hypernucleus with a binding energy and width of 4.4 MeV and 3 MeV (σ), respectively. Therefore, confirming this bound $\Sigma^0 nn$ becomes very interesting and important.

In summary, this experiment demonstrated that the $(e, e'K^+)$ reaction is a unique tool to investigate the possibility of 3-body neutral Λ and Σ hypernuclei with high precision using a pressurized tritium gas target. A ${}^3_\Lambda n$ resonance and a pair of ${}^3_\Sigma N$ states were possibly observed. However, to make a definitive identification, improved statistics are required. At JLab, these highly interesting and important systems can be studied precisely. An experiment with optimized apparatus and kinematics (low-

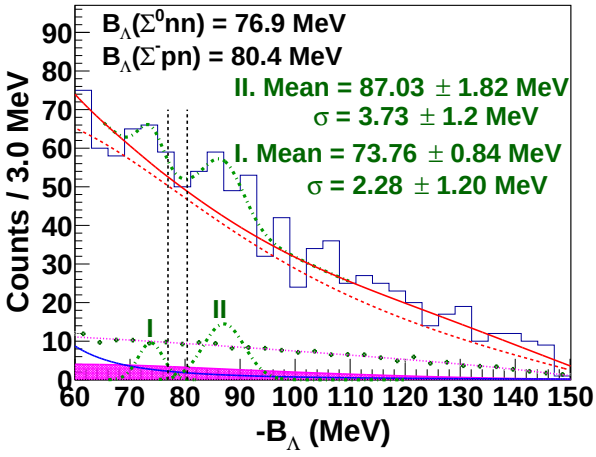

FIG. 6. (Color online) The enlarged mass spectrum plotted with a larger bin size (3.0 MeV/bin) in terms of the binding energy B_Λ of the ${}^3_\Lambda n$ hypernucleus. The $\Sigma^- d$ threshold is in between the two listed ΣNN thresholds and ignored here.

ering the 3-momentum transfer to the Λ) can increase the production yield by a factor of about 20 while reducing the background by at least a factor of 3. Statistical uncertainties would be significantly improved.

ACKNOWLEDGMENTS

We acknowledge the support given by the JLab staff and engineers from the Physics and Accelerator Divisions and the outstanding contribution of the Jefferson Lab target group for the design and safe handling of the tritium target for the present experiment. We also thank E. Hiyama, T. Mart, T. Motoba, K. Miyagawa, and M. Schäfer for extensive discussions. This work was supported by the U.S. Department of Energy (DOE) grant DE-AC05-06OR23177 under which Jefferson Science Associates, LLC, operates the Thomas Jefferson National Accelerator Facility. We acknowledge the support by the DOE grants DE-FG02-97ER41047 and DE-AC02-06CH11357, and by the U.S. National Science Foundation grant PHY-1714809. This work was partially supported by the Grant-in-Aid for Scientific Research on Innovative Areas "Toward new frontiers Encounter and synergy of state-of-the-art astronomical detectors and exotic quantum beams." The work was supported by JSPS KAKENHI Grants No. 18H05459, No. 18H05457, No. 18H01219, No. 17H01121, and 19J22055. The work was also supported by SPIRITS 2020 of Kyoto University, and the Graduate Program on Physics for the Universe, Tohoku University (GP-PU).

[1] Th. A. Rijken, V. G. J. Stoks, and Y. Yamamoto, Phys. Rev. C **59**, 21 (1999).
[2] Th. A. Rijken and Y. Yamamoto, Phys. Rev. C **73**, 044008 (2006).
[3] Th. A. Rijken, M. M. Nagels, and Y. Yamamoto, Nucl. Phys. A **835**, 160 (2010).
[4] Y. Yamamoto and Th. A. Rijken, Few-Body Syst. **54**, 57 (2013).
[5] J. Haidenbauer and Ulf-G. Meissner, Phys. Rev. C **72**, 044005 (2005).
[6] J. Haidenbauer, S. Petschauer, N. Kaiser, U.-G. Meissner, A. Nogga, and W. Weise, Nucl. Phys. A **915**, 24 (2013).
[7] F. Schulz, P. Achenbach, S. Aulenbacher, J. Beričič, S. Bleser, R. Böhm, *et al.*, Nucl. Phys. A **954**, 149 (2016).
[8] A. Esser, S. Nagao, F. Schulz, P. Achenbach, C. Ayerbe-Gayoso, R. Bohm, *et al.*, Phys. Rev. Lett. **114**, 232501 (2015).
[9] T. O. Yamamoto, M. Agnello, Y. Akazawa, N. Amano, K. Aoki, E. Botta, *et al.*, Phys. Rev. Lett. **115**, 222501 (2015).
[10] C. Rappold, E. Kim, T. R. Saito, O. Bertini, S. Bianchin, V. Bozkurt, *et al.*, Phys. Rev. C **88**, 041001(R) (2013).
[11] H. Garcilazo and A. Valcarce, Phys. Rev. C **89**, 057001 (2014).
[12] E. Hiyama, S. Ohnishi, B. F. Gibson, and Th. A. Rijken, Phys. Rev. C **89**, 061302(R) (2014).
[13] A. Gal and H. Garcilazo, Phys. Lett. **B** 736, 93 (2014).
[14] I. R. Afnan and B. F. Gibson, Phys. Rev. C **92**, 054608 (2015).
[15] I. R. Afnan and B. F. Gibson, Few-Body Systems **60**, 3, 51 (2019).
[16] K. N. Suzuki, T. Gogami, B. Pandey, K. Itabashi, S. Nagao, K. Okuyama, *et al.*, Progress of Theoretical and Experimental Physics, Volume **2022**, 013D01 (2022).
[17] J. Alcorn *et al.*, Nucl. Instr. and Meth., A **522**, Issue **3**, 249-346 (2004).
[18] S. N. Santiesteban *et al.*, Nucl. Instr. and Meth., A **940**, 351-358 (2019).
[19] L. Tang, C. Chen, T. Gogami, D. Kawama, Y. Han, L. Yuan, *et al.*, Phys. Rev. C **90**, 034320 (2014).
[20] C. Ciofi degli Atti and S. Simula, Phys. Rev. C **53**, 1689-1710 (1996).
[21] T. Harada and Y. Hirabayashi, Phys. Rev. C **89**, 054603 (2014).
[22] T. Nagae, T. Miyachi, T. Fukuda, H. Outa, T. Tamagawa, J. Nakano, *et al.*, Phys. Rev. Lett. **80**, 1605-1609 (1998).